

# Hydrogen-Bonded Complexes of Aromatic Crown Ethers with (9-Anthracenyl)methylammonium Derivatives. Supramolecular Photochemistry and Photophysics. pH-Controllable Supramolecular Switching<sup>†</sup>

Peter R. Ashton,<sup>‡</sup> Roberto Ballardini,<sup>\*,§</sup> Vincenzo Balzani,<sup>\*,||</sup> Marcos Gómez-López,<sup>‡,⊥</sup> Simon E. Lawrence,<sup>#</sup> M. Victoria Martínez-Díaz,<sup>‡</sup> Marco Montalti,<sup>||</sup> Arianna Piersanti,<sup>||</sup> Luca Prodi,<sup>§</sup> J. Fraser Stoddart,<sup>\*,‡,⊥</sup> and David J. Williams<sup>\*,#</sup>

Contribution from Istituto FRAE-CNR, via Gobetti 101, 40129 Bologna, Italy, Dipartimento di Chimica "G. Ciamician" dell'Università, via Selmi 2, I-40126, Bologna, Italy, The School of Chemistry, The University of Birmingham, Edgbaston, Birmingham B15 2TT, UK, and The Department of Chemistry, Imperial College, South Kensington, London SW7 2AY, UK

Received May 15, 1997<sup>⊗</sup>

**Abstract:** The (9-anthracenyl)methylammonium and (9-anthracenyl)benzylammonium tetrakis(hexafluorophosphate) salts give hydrogen-bonded complexes in CH<sub>2</sub>Cl<sub>2</sub> with aromatic crown ethers containing dibenzo (**DB**) or dinaphtho (**DN**) units. The association constants vary from  $3 \times 10^3$  to  $1 \times 10^6$  M<sup>-1</sup> in CH<sub>2</sub>Cl<sub>2</sub>, depending on the specific ammonium cation and crown ether involved. In a number of cases, pseudorotaxane-like geometries for the complexes are demonstrated by (a) <sup>1</sup>H NMR spectroscopy in solution, (b) X-ray crystallography in the solid state, and (c) mass spectrometry in the gas phase. The results obtained by absorption, emission, and excitation spectroscopy and excited lifetimes show that, as a consequence of the hydrogen bond driven recognition process, the anthracene chromophoric unit interacts with the aromatic units of the crown ethers. In the complexes involving the **DB18C6**, **DB24C8**, and **DB30C10** macrocycles, the interaction leads to the complete quenching of the fluorescence of the dialkoxybenzene moieties and parallels sensitization of the anthracene fluorescence. In the complexes of **1/5-DN38C10**, both the crown and the anthracene fluorescence are completely quenched, most likely by an energy-transfer cascade involving the triplet state of the dialkoxynaphthalene moiety. In the complexes of **2/3-DN30C10**, the interaction between the anthracene moiety and the naphthalene rings of the crown ether is relatively strong, as indicated by the perturbation of the absorption bands, the disappearance of the fluorescence bands of the naphthalene- and anthracene-type chromophoric units, and the appearance of a new, broad fluorescence band. The complexes can also be formed by addition of CF<sub>3</sub>COOH or CF<sub>3</sub>SO<sub>3</sub>H to CH<sub>2</sub>Cl<sub>2</sub> solutions containing crown ether and amine. The association process between **DB24C8** and (9-anthracenyl)benzylammonium salt can be reversed quantitatively upon addition of a suitable base and the complex can be formed again after treatment with acid.

## Introduction

Much attention<sup>1</sup> is being devoted currently to the interaction between light and designed supramolecular systems, a number of which exploit the energy and/or information content of photons.<sup>2</sup> This exploitation can be achieved by two different routes.<sup>2a,e</sup> The first route ("photon writing") involves a photochemical reaction occurring in a supramolecular system that causes ("writes") some changes in the properties of the system which

are reflected in a monitorable signal. The second one ("photon reading") is based on an interaction between components of a supramolecular system which affects their photon response, such that the occurrence of the interaction can be revealed ("read") by some form of excited state manifestation—usually luminescence. In host–guest complexes, the photochemical and photophysical properties of each component can be modified profoundly upon complexation. Such changes can be useful in obtaining information on the structure of a complex and also in assisting the design of sensors for a variety of applications.

It is well-known that crown ethers can form complexes with RNH<sub>3</sub><sup>+</sup> ions.<sup>3–5</sup> More recently, it has been shown that suitably chosen R<sub>2</sub>NH<sub>2</sub><sup>+</sup> ions can thread through the cavities of appropriately constituted crown ethers to give inclusion complexes with pseudorotaxane-like geometries.<sup>6,7</sup> Our interest in the development of photochemical molecular and supramolecular

<sup>†</sup> Molecular Meccano, part 26. For part 25, see: Belohradsky, M.; Hamers, C.; Menzer, S.; Raymo, F. M.; Shipway, A. N.; Stoddart, J. F.; White, A. J. P.; Williams, D. J. *Macromolecules*, submitted.

<sup>‡</sup> University of Birmingham.

<sup>§</sup> Istituto FRAE-CNR.

<sup>||</sup> Università di Bologna.

<sup>⊥</sup> Address for correspondence: Department of Chemistry and Biochemistry, University of California at Los Angeles, 405 Hilgard Avenue, Los Angeles, CA 90095. E-mail: stoddart@chem.ucla.edu.

<sup>#</sup> Imperial College.

<sup>⊗</sup> Abstract published in *Advance ACS Abstracts*, October 1, 1997.

(1) (a) Balzani, V.; Scandola, F. *Supramolecular Photochemistry*; Horwood: Chichester, 1991. (b) Balzani, V. *Tetrahedron* **1992**, *48*, 10443–10514. (c) Wasielewski, M. R.; O'Neil, M. P.; Gosztola, D.; Niemczyk, M. P.; Svec, W. A. *Pure Appl. Chem.* **1992**, *64*, 1319–1325. (d) Bissell, R. A.; de Silva, A. P.; Gunaratne, H. Q. N.; Lynch, P. L. M.; Maguire, G. E. M.; McCoy, C. P.; Sandanayake, K. R. A. S. *Top. Curr. Chem.* **1993**, *168*, 223–264. (e) Fabbrizzi, L.; Poggi, A. *Chem. Soc. Rev.* **1995**, *24*, 197–202. (f) Lehn, J.-M. *Supramolecular Chemistry: Concepts and Perspectives*; VCH: Weinheim, 1995.

(2) (a) Balzani, V.; Scandola, F. In *Comprehensive Supramolecular Chemistry*; Reinhoudt, D. N., Ed.; Pergamon Press: Oxford, England, 1996; Vol. 10, pp 687–746. (b) Feringa, L. B.; Jager, W. F.; de Lange, B. *Tetrahedron* **1993**, *49*, 8267–8309. (c) de Silva, A. P.; McCoy, C. P. *Chem. Ind.* **1994**, *24*, 992–996. (d) de Silva, A. P.; Gunaratne, H. Q. N.; Gunlaugsson, T.; Huxley, A. J. M.; McCoy, C. P.; Rademacher, J. T.; Rice, T. E. *Chem. Rev.* **1997**, *97*, 1515–1566. (e) Scandola, F.; Bignozzi, C. A.; Balzani, V. *Chim. Ind. (Milan)* **1995**, *78*, 1221–1231. (f) Balzani, V.; Credi, A.; Scandola, F. *Chim. Ind. (Milan)* **1997**, *79*, 751–759.

(3) Pedersen, C. J. *J. Am. Chem. Soc.* **1967**, *89*, 7017–7036.

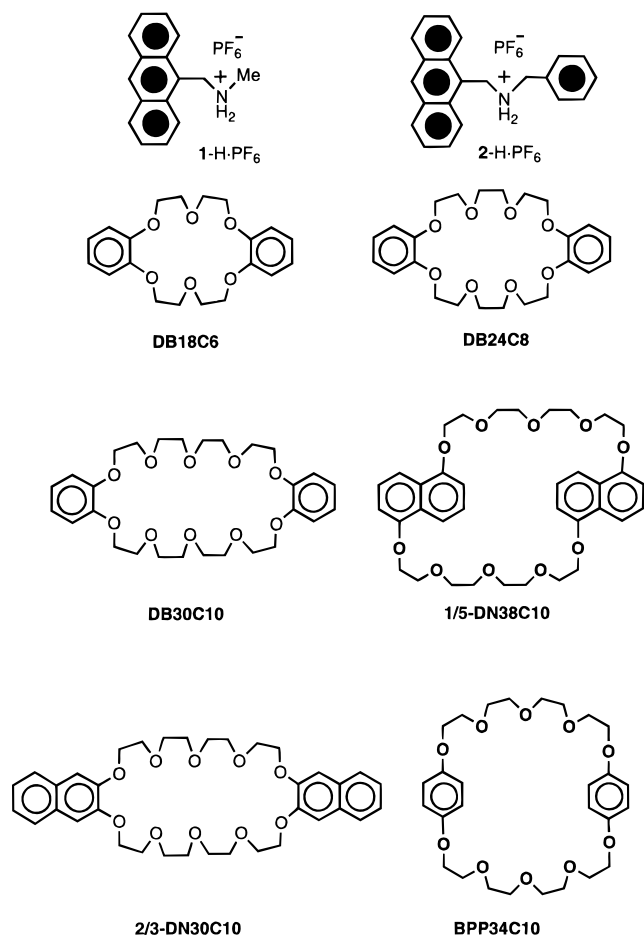


**Figure 1.** Formulas of the compounds and abbreviations used.

devices,<sup>8</sup> together with recent studies on photoinduced energy- and electron-transfer processes in supramolecular systems based

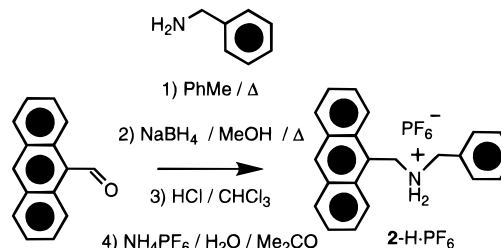
(4) (a) Shinkai, S.; Ishihara, M.; Ueda, K.; Manabe, O. *J. Chem. Soc., Perkin Trans. 2* **1985**, 511–518. (b) Sutherland, I. O. *Chem. Soc. Rev.* **1986**, 15, 63–91. (c) Stoddart, J. F. *Top. Stereochem.* **1988**, 17, 207–288. (d) Gokel, G. W. *Crown Ethers and Cryptands*; The Royal Society of Chemistry: London, 1991. (e) Lindoy, L. F. *The Chemistry of Macrocyclic Ligands*; Cambridge University Press: Cambridge, 1989. (f) Izatt, R. M.; Pawlak, K.; Bradshaw, J. S.; Bruening, R. L. *Chem. Rev.* **1995**, 95, 2529–2586.

(5) For interesting applications, see: (a) Izatt, R. M.; Nielsen B. L.; Christensen, J. J.; Lamb, J. D. *J. Membrane Sci.* **1981**, 9, 263–271. (b) Reetz, M. T.; Huff, J.; Rudolf, J.; Toeller, K.; Deege, A.; Goddard, R. *J. Am. Chem. Soc.* **1994**, 116, 11588–11584. (c) Izatt, R. M.; Wang, T.; Hathaway, J. K.; Zhang, X. X.; Curtis, J. C.; Bradshaw, J. S.; Zhu, C. Y.; Huszthy, P. *J. Inclusion Phenom.* **1994**, 17, 157–175 and references therein.

(6) Kolchinski, A. G.; Busch, D. H.; Alcock, N. W. *J. Chem. Soc., Chem. Commun.* **1995**, 1289–1291.

(7) (a) Ashton, P. R.; Campbell, P. J.; Chrystal, E. J. T.; Glink, P. T.; Menzer, S.; Philp, D.; Spencer, N.; Stoddart, J. F.; Tasker, P. A.; Williams, D. *J. Angew. Chem., Int. Ed. Engl.* **1995**, 34, 1865–1869. (b) Ashton, P. R.; Chrystal, E. J. T.; Glink, P. T.; Menzer, S.; Schiavo, C.; Stoddart, J. F.; Tasker, P. A.; Williams, D. *J. Angew. Chem., Int. Ed. Engl.* **1995**, 34, 1869–1871. (c) Glink, P. T.; Schiavo, C.; Stoddart, J. F.; Williams, D. *J. Chem. Commun.* **1996**, 1483–1490. (d) Ashton, P. R.; Chrystal, E. J. T.; Glink, P. T.; Menzer, S.; Schiavo, C.; Spencer, N.; Stoddart, J. F.; Tasker, P. A.; White, A. J. P.; Williams, D. *J. Chem. Eur. J.* **1996**, 2, 709–728. (e) Ashton, P. R.; Glink, P. T.; Stoddart, J. F.; Tasker, P. A.; White, A. J. P.; Williams, D. *J. Chem. Eur. J.* **1996**, 2, 729–736. (f) Ashton, P. R.; Glink, P. T.; Martínez-Díaz, M.-V.; Stoddart, J. F.; White, J. P.; Williams, D. *J. Angew. Chem., Int. Ed. Engl.* **1996**, 35, 1930–1933. (g) Ashton, P. R.; Glink, P. T.; Menzer, S.; Stoddart, J. F.; Tasker, P. A.; White, A. J. P.; Williams, D. *J. Tetrahedron Lett.* **1996**, 37, 6217–6220. (h) Ashton, P. R.; Collins, A. N.; Fyfe, M. C. T.; Glink, P. T.; Menzer, S.; Stoddart, J. F.; Williams, D. *J. Angew. Chem., Int. Ed. Engl.* **1997**, 36, 59–62. (i) Ashton, P. R.; Collins, A. N.; Fyfe, M. C. T.; Menzer, S.; Stoddart, J. F.; Williams, D. *J. Angew. Chem., Int. Ed. Engl.* **1997**, 36, 735–739. (j) Feiters, M. C.; Fyfe, M. C. T.; Martínez-Díaz, M.-V.; Menzer, S.; Nolte, R. J. M.; Stoddart, J. F.; Van Kan, P. J. M.; Williams, D. *J. Am. Chem. Soc.* **1997**, 119, 8119–8120.

## Scheme 1



on hydrogen bonds,<sup>9</sup> has led us to explore whether interactions between crown ethers and  $RR'NH_2^+$  ions can be exploited in the design of systems of both photochemical and photophysical interest. Thus, we have chosen two  $RR'NH_2^+$  ions and a range of aromatic crown ethers, both exhibiting fluorescence properties, and studied the photoinduced processes that take place in their complexes. Their structural features have been studied by (a) X-ray crystallography in the solid state, (b)  $^1H$  NMR spectroscopy in solution, and (c) mass spectrometry in the gas phase. Finally, we describe in one of the 1:1 complexes a reversible base-induced decomplexation process which can be monitored by both  $^1H$  NMR spectroscopy and luminescence studies.

## Results and Discussion

**Synthesis.** We have targeted the formation of inclusion complexes between the salts **1-H-PF<sub>6</sub>** and **2-H-PF<sub>6</sub>**, both containing a photosensitizer—an anthracene unit—as the terminal substituent, and **DB18C6**, **DB24C8**, **DB30C10**, **1/5-DN38C10**, **2/3-DN30C10**, and **BPP34C10** as the macrocyclic components (Figure 1). The amine precursor to the **1-H-PF<sub>6</sub>** salt is commercially available and the (9-anthracenyl)methylbenzylammonium hexafluorophosphate **2-H-PF<sub>6</sub>** was readily prepared<sup>7b</sup> as follows (Scheme 1). Condensation of 9-anthraldehyde with  $PhCH_2NH_2$ , followed by reduction ( $NaBH_4/MeOH$ ) of the imine, yielded **2**, which, after treatment with concentrated HCl followed by counterion exchange ( $NH_4PF_6/H_2O/Me_2CO$ ), afforded the pure salt **2-H-PF<sub>6</sub>**.

**Photophysical Properties of the Components.** The absorption and emission properties of the components are summarized in Table 1. The absorption and emission spectra of **2-H-PF<sub>6</sub>** and of the crown ethers **DB24C8** and **1/5-DN38C10** are shown in Figures 2 and 3. The absorption spectrum<sup>10</sup> of **2-H-PF<sub>6</sub>**,

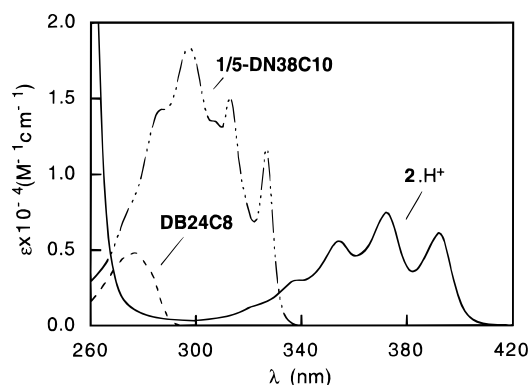
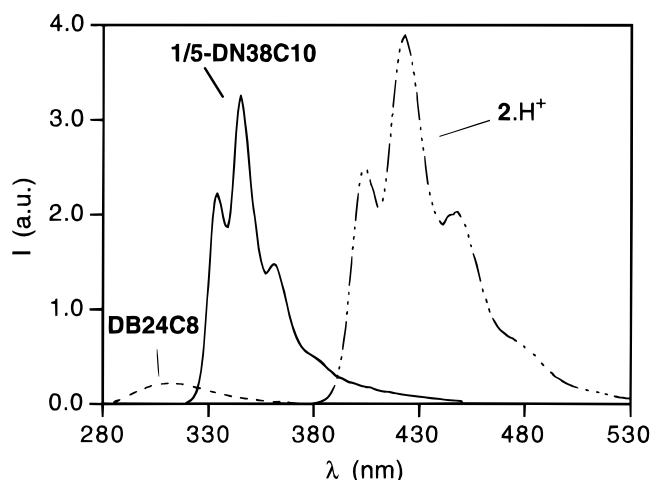
(8) (a) Balzani, V.; Moggi, L.; Scandola, F. in *Supramolecular Photochemistry*; Balzani, V., Ed.; Reidel: Dordrecht, 1987; pp 1–28. (b) Balzani, V.; Scandola, F. *Supramolecular Photochemistry*; Horwood: Chichester, 1991; Chapter 12. (c) Campagna, S.; Denti, G.; Serroni, S.; Juris, A.; Venturi, M.; Ricevuto, V.; Balzani, V. *Chem. Eur. J.* **1995**, 1, 211–221. (d) Barigelletti, F.; Flamigni, L.; Balzani, V.; Collin, J.-P.; Sauvage, J.-P.; Sour, A. *New J. Chem.* **1995**, 19, 793–798. (e) Parola, A. J.; Pina, F.; Ferreira, E.; Maestri, M.; Balzani, V.; *J. Am. Chem. Soc.* **1996**, 118, 11610–11616. (f) Gómez-López, M.; Preece, J. A.; Stoddart, J. F. *Nanotechnology* **1996**, 7, 183–192. (g) Ashton, P. R.; Ballardini, R.; Balzani, V.; Boyd, S. E.; Credi, A.; Gandolfi, M. T.; Gómez-López, M.; Iqbal, S.; Philp, D.; Preece, J. A.; Prodi, L.; Ricketts, H. G.; Stoddart, J. F.; Tolley, M. S.; Venturi, M.; White, A. J. P.; Williams, D. *J. Chem. Eur. J.* **1997**, 3, 152–170. (h) Credi, A.; Balzani, V.; Langford, S. J.; Stoddart, J. F. *J. Am. Chem. Soc.* **1997**, 119, 2679–2681. (i) Pina, F.; Melo, M. J.; Maestri, M.; Ballardini, R.; Balzani, V. *J. Am. Chem. Soc.* **1997**, 119, 2679–2681. (j) Murakami, H.; Kawabuchi, A.; Kotoo, K.; Kunitake, M.; Nakashima, N. *J. Am. Chem. Soc.* **1997**, 119, 7605–7606.

(9) (a) Aoyama, Y.; Asakawa, M.; Matsui, Y.; Ogoshi, H. *J. Am. Chem. Soc.* **1991**, 113, 6233–6240. (b) Král, V.; Springs, S. L.; Sessler, J. L. *J. Am. Chem. Soc.* **1995**, 117, 8881–8882. (c) Roberts, J. A.; Kirby, J. P.; Nocera, D. G. *J. Am. Chem. Soc.* **1995**, 117, 8051–8052. (d) Lewis, F. D.; Yang, J.-S.; Stern, C. L. *J. Am. Chem. Soc.* **1996**, 118, 2772–2773. (e) Arimura, T.; Brown, C. T.; Springs, S. L.; Sessler, J. L. *Chem. Commun.* **1996**, 2293–2294.

(10) Montalti, M.; Ballardini, R.; Prodi, L.; Balzani, V. *Chem. Commun.* **1996**, 2011–2012.

**Table 1.** Absorption and Emission Properties in CH<sub>2</sub>Cl<sub>2</sub> Solution at 298 K

	absorption		fluorescence		
	$\lambda_{\max}$ (nm)	$\epsilon$ (M <sup>-1</sup> cm <sup>-1</sup> )	$\lambda_{\max}$ (nm)	$I_{\text{rel}}$	$\tau$ (ns)
1-H <sup>+</sup>	372	6000	421	100	12.0
2-H <sup>+</sup>	372	7400	423	82	10.0
DB18C6	277	4900	310	4	0.5
DB24C8	277	5100	312	5	0.5
DB30C10	277	4600	312	5	0.5
1/5-DN38C10	297	16500	345	68	8.0
2/3-DN30C10	268	8800	342	104	9.6

**Figure 2.** Absorption spectra of the protonated derivative 2-H<sup>+</sup> and of the crown ethers DB24C8 and 1/5-DN38C10 in CH<sub>2</sub>Cl<sub>2</sub> solution at 298 K.**Figure 3.** Emission spectra of the derivative 2-H<sup>+</sup> and of the crown ethers DB24C8 and 1/5-DN38C10 in CH<sub>2</sub>Cl<sub>2</sub> solution at 298 K.

which above 270 nm is very similar to that of 1-H·PF<sub>6</sub>, shows the characteristic structured bands of the anthracene chromophoric unit.<sup>11</sup> The absorption spectrum of crown ether DB24C8, which is practically identical to those of crown ethers DB18C6 and DB30C10, shows the characteristic band for the 1,2-dimethoxybenzene chromophoric units.<sup>12a</sup> The absorption spectrum of crown ether 1/5-DN38C10 shows the characteristic bands of the naphthalene-type compounds.<sup>11</sup> As expected, the

(11) (a) Murov, S. L.; Carmichael, I.; Hug, G. L. *Handbook of Photochemistry*; Dekker: New York, 1993. (b) Berlman, I. B. *Handbook of Fluorescence Spectra of Aromatic Compounds*; Academic Press: London, 1965. (c) Jaffé, H. H.; Orchin, M. *Theory and Applications of Ultraviolet Spectroscopy*; Wiley: New York, 1964.

(12) (a) Anelli, P. L.; Ashton, P. R.; Ballardini, R.; Balzani, V.; Delgado, M.; Gandolfi, M. T.; Goodnow, T. T.; Kaifer, A. E.; Philp, D.; Pietraszkiewicz, M.; Prodi, L.; Reddington, M. V.; Slawin, A. M. Z.; Spencer, N.; Stoddart, J. F.; Vicent, C.; Williams, D. J. *J. Am. Chem. Soc.* **1992**, *114*, 193–218. (b) Ballardini, R.; Gandolfi, M. T.; Prodi, L.; Ciano, M.; Balzani, V.; Kohnke, F.; Shariari-Zavariah, H.; Spencer, N.; Stoddart, J. F. *J. Am. Chem. Soc.* **1989**, *111*, 7072–7078.

**Table 2.** Association Constants ( $K_a$ , M<sup>-1</sup>) in CH<sub>2</sub>Cl<sub>2</sub> at 298 K<sup>a</sup>

	DB18C6	DB24C8	DB30C10	1/5-DN38C10	2/3-DN30C10
1-H <sup>+</sup>	$1.4 \times 10^4$	$1.0 \times 10^5$	$7.0 \times 10^4$	$5.0 \times 10^3$	$4.0 \times 10^5$
2-H <sup>+</sup>	$3.0 \times 10^3$	$1.0 \times 10^6$	$2.0 \times 10^5$	$7.0 \times 10^3$	$4.0 \times 10^5$

<sup>a</sup> Obtained by spectrofluorimetric measurements.

spectrum of crown ether 2/3-DN30C10 is slightly different than that of 1/5-DN38C10, because of the difference between the 2,3- and 1,5-dimethoxynaphthalene units.<sup>12b</sup>

It is well-known<sup>1d</sup> that amines linked covalently to anthracene quench its fluorescence by intramolecular electron transfer involving the lone pair on the amino group. When the amino group is protonated, the quenching process is prevented and the strong, structured fluorescence band of the anthracene unit<sup>11</sup> is present. The fluorescence spectrum (Figure 3) of 2-H·PF<sub>6</sub> shows such a structured fluorescence band. The fluorescence spectrum of 1-H·PF<sub>6</sub> is very similar to that of 2-H·PF<sub>6</sub> (Table 1).

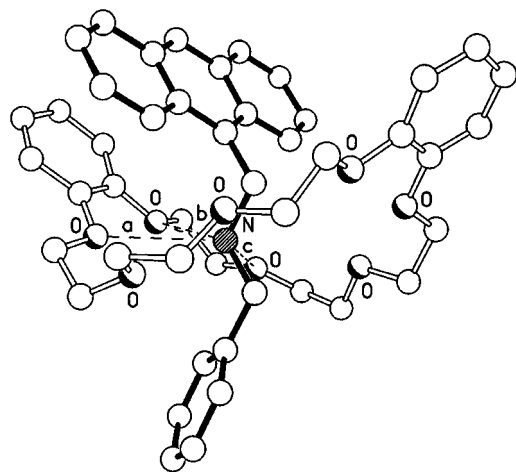
Each crown ether exhibits (Table 1) an intense and short-lived fluorescence. The fluorescence spectra of DB24C8 and 1/5-DN38C10 are shown in Figure 3. In a rigid matrix at 77 K, the crown ethers also show a relatively strong phosphorescence band.

**Complex Formation.** When the amine precursors of 1-H·PF<sub>6</sub> and 2-H·PF<sub>6</sub> are dissolved in CH<sub>2</sub>Cl<sub>2</sub> solutions of the crown ethers, no change is observed in the spectra compared with those for the separate species. However, when the amine precursors 1 and 2 are replaced by the PF<sub>6</sub><sup>-</sup> salts 1-H·PF<sub>6</sub> and 2-H·PF<sub>6</sub>, strong changes in the fluorescence properties (and, in one case, also in the absorption spectrum, *vide infra*) are observed. Such changes indicate that complexes are being formed in which the chromophoric groups of the protonated amines and crown ethers undergo electronic interaction.

It is generally observed that, in CH<sub>2</sub>Cl<sub>2</sub> solution, the fluorescence intensities of the crown ethers decrease, up to complete disappearance, on addition of 1-H·PF<sub>6</sub> or 2-H·PF<sub>6</sub>. Under the experimental conditions used for the photophysical experiments, the predominant species were 1:1 complexes in all cases. The  $K_a$  values obtained (Table 2) vary from  $3 \times 10^3$  to  $1 \times 10^6$  M<sup>-1</sup>, depending on the specific ammonium ion and crown ether involved.

Qualitatively similar changes in the fluorescence spectra can be observed when CF<sub>3</sub>COOH or CF<sub>3</sub>SO<sub>3</sub>H are added to CH<sub>2</sub>Cl<sub>2</sub> solutions containing a crown ether and the amines 1 or 2. This observation confirms that a necessary condition for complex formation is the protonation of the amines. A role is also played, however, by the counterion of the protonated amines. In the case of CF<sub>3</sub>SO<sub>3</sub><sup>-</sup>, the association constant of the complex is considerably smaller than that for PF<sub>6</sub><sup>-</sup> (e.g.,  $2 \times 10^4$  M<sup>-1</sup> for 2-H·CF<sub>3</sub>SO<sub>3</sub> with DB24C8). In the case of CF<sub>3</sub>COO<sup>-</sup>, we have found<sup>10</sup> previously that formation of a complex between the protonated amine and the counterion competes favorably with the formation of the complex between the protonated amine and the crown ether, so that the formation of the latter complex begins only after addition of more than one equivalent of acid. In all cases, the spectral changes can be fully reversed upon the addition of a suitable base like tributylamine.

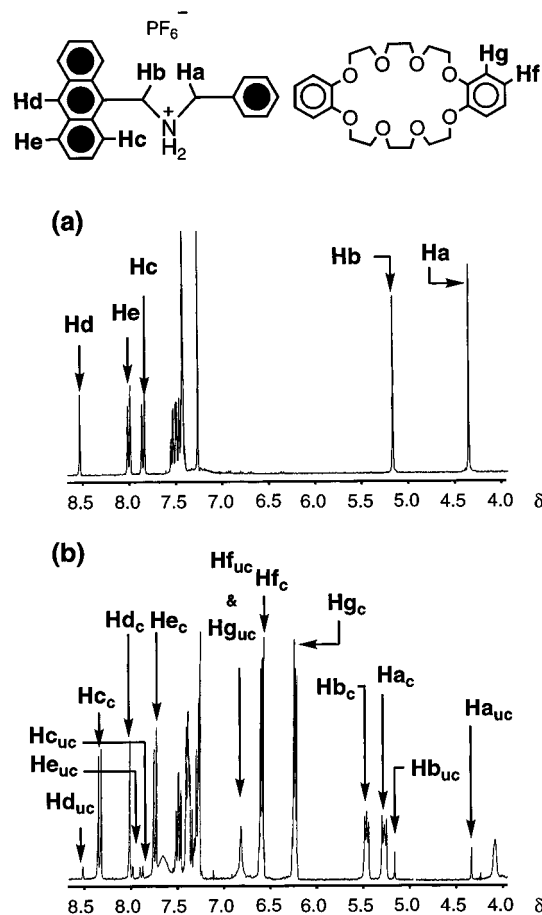
**X-ray Crystallography: Complexes between 2-H·PF<sub>6</sub> and the Crown Ether DB24C8 in the Solid State.** The solid state structure (Figure 4) of the 1:1 complex formed between the DB24C8 and 2-H·PF<sub>6</sub> shows there to be two independent virtually identical 1:1 complexes (A and B) in the crystal. In each case, the cation is threaded through the centers of the DB24C8 macrocycles, the 1:1 complexes being stabilized by a



**Figure 4.** The solid state superstructure of one (A) of the pairs of crystallographically-independent 1:1 complexes, formed between **DB24C8** and **2-H<sup>+</sup>PF<sub>6</sub><sup>-</sup>**, showing the intercomponent [N<sup>+</sup>—H···O] hydrogen bonding and  $\pi$ - $\pi$  stacking interactions. Hydrogen bonding geometries: [N<sup>+</sup>···O], [H···O] distances (Å), [N<sup>+</sup>—H···O] angles (deg), (a) 3.15, 2.15, 150; (b) 3.02, 2.35, 126; (c) 3.15, 2.23, 159. The equivalent hydrogen bonding geometries in the other (B) independent complex are (a) 2.98, 2.09, 154; (b) 3.01, 2.36, 125; (c) 3.04, 2.14, 157.

combination of [N<sup>+</sup>—H···O] hydrogen bonds between the ammonium hydrogen atoms of the guest and the polyether oxygen atoms of the host, and a face-to-face  $\pi$ - $\pi$  stacking interaction between one of the catechol rings of the **DB24C8** and the anthracenyl ring of the cation **2-H<sup>+</sup>PF<sub>6</sub><sup>-</sup>**. In complex A, the catechol and the anthracenyl rings are inclined by *ca.* 3° and have a mean interplanar separation of 3.47 Å; in complex B, these parameters are 2° and 3.50 Å, respectively. The only significant difference between the two complexes, A and B, is in the conformation adopted by the two cations. In both complexes, the C—CH<sub>2</sub>—NH<sub>2</sub><sup>+</sup>—CH<sub>2</sub>—C backbones adopt an *all-anti* geometry that is coplanar to better than 0.1 Å. Although the plane of the anthracenyl ring system is, in each case, inclined by 88° to the plane of the backbone, the phenyl rings adopt differing twist angles of 44° and 27° in complexes A and B, respectively. Inspection of the packing of the 1:1 complexes reveals a chain of aromatic—aromatic edge-to-face interactions “linking” complexes A and B throughout the crystal. One of these interactions involves the edge of a catechol ring of one complex (A) and the face of one of the terminal six-membered rings of the anthracenyl ring in the neighboring complex (B) (the associated [H··· $\pi$ ] distance and [C—H··· $\pi$ ] angle are 2.79 Å and 68°). The other edge-to-face interaction is between the edge of one of the catechol rings in complex B and the face of the  $\pi$ -stacked catechol ring in complex A. Here, the [H··· $\pi$ ] distance and [C—H··· $\pi$ ] angle are 2.92 Å and 163°, respectively.

**<sup>1</sup>H NMR Spectroscopy: Formation of the Complexes between 2-H<sup>+</sup>PF<sub>6</sub><sup>-</sup> and the Crown Ether DB24C8 in Solution.** The addition of equimolar amounts of the crown ether **DB24C8** to a solution of **2-H<sup>+</sup>PF<sub>6</sub><sup>-</sup>** in a mixture of CDCl<sub>3</sub> and CD<sub>3</sub>CN (6:1, v/v) at 25 °C produces significant shifts in the <sup>1</sup>H NMR signals assigned to both of the components. The <sup>1</sup>H NMR spectra of **2-H<sup>+</sup>PF<sub>6</sub><sup>-</sup>** in its free form and of an equimolar mixture of **2-H<sup>+</sup>PF<sub>6</sub><sup>-</sup>** and **DB24C8** in a solution of CDCl<sub>3</sub> and CD<sub>3</sub>CN (6:1, v/v) at 25 °C are shown in parts a and b of Figure 5, respectively. The assignments of the resonances are based on NOE experiments. The spectrum of **2-H<sup>+</sup>PF<sub>6</sub><sup>-</sup>**, recorded in the presence of **DB24C8**, shows (Figure 5b) distinguishable sets of resonances for (1) free **2-H<sup>+</sup>PF<sub>6</sub><sup>-</sup>**, (2) free **DB24C8** and (3) the 1:1 complex between the crown ether and the RR'NH<sub>2</sub><sup>+</sup> ion, indicating that the kinetics of the complexation and

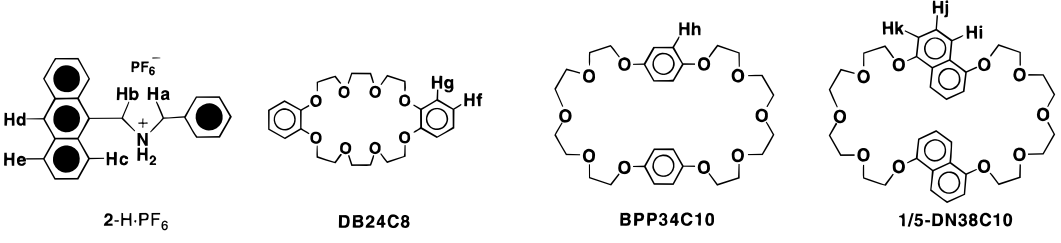


**Figure 5.** <sup>1</sup>H NMR (300 MHz, CDCl<sub>3</sub>/MeCN, 6:1) spectra of (a) the dialkylammonium salt **2-H<sup>+</sup>PF<sub>6</sub><sup>-</sup>** and (b) of a 1:1 mixture of **2-H<sup>+</sup>PF<sub>6</sub><sup>-</sup>** and **DB24C8**, showing signals for both complexed (indicated on the Figure with c) and uncomplexed (indicated on the Figure with uc) species.

decomplexation processes are both slow on the <sup>1</sup>H NMR (300 MHz) time scale at room temperature.

The <sup>1</sup>H NMR chemical shifts ( $\delta$  values) for the different components (**DB24C8**, **BPP34C10**, **1/5-DN38C10**, and **2-H<sup>+</sup>PF<sub>6</sub><sup>-</sup>**) and of their changes ( $\Delta\delta$  values) upon complexation are reported in Table 3. In the case of **DB24C8**, large downfield shifts are detectable for the methylene protons (**Ha** and **Hb**) adjacent to the NH<sub>2</sub><sup>+</sup> center. Since similar downfield shifts have already been reported<sup>7a</sup> for the formation of pseudorotaxane complexes between the dibenzylammonium cation and **DB24C8**; this result suggests the formation of a 1:1 complex with a pseudorotaxane-like geometry in this case as well.

The  $\Delta\delta$  value ( $\Delta\delta = 0.93$  ppm) for the benzylic methylene protons is larger than that ( $\Delta\delta = 0.30$  ppm) for the anthracenylmethyl protons, suggesting that, while the benzylic methylene group can penetrate into the cavity of the **DB24C8**, the anthracenylmethyl group cannot because of the steric hindrance of the proximal 9-substituted anthracene moiety.<sup>6</sup> However, upon complexation, while the resonance assigned to the **Hc** proton of the anthracenyl group becomes strongly deshielded, the signals assigned to the **Hd** and **He** protons become shielded. Furthermore, the protons located on the macrocyclic polyether's catechol ring resonate as two sets of signals that are shifted strongly upfield with respect to the signal associated with the uncomplexed crown ether as a consequence of the  $\pi$ - $\pi$  stacking interactions between the anthracene moiety of the guest and the catechol rings of the host (Figure 4). A bidimensional NOE experiment was undertaken on an equimolar mixture of **2-H<sup>+</sup>PF<sub>6</sub><sup>-</sup>** and **DB24C8** in CDCl<sub>3</sub> and CD<sub>3</sub>CN (6:1, v/v) as solvent

**Table 3.** Chemical Shifts ( $\delta$  values) and Chemical Shift Changes ( $\Delta\delta$  values) in the  $^1\text{H}$  NMR (300 MHz,  $\text{CHCl}_3/\text{MeCN}$ , 6:1, rt) Spectral Data of the Dialkylammonium Salt  $2\text{-H}\cdot\text{PF}_6$  with 1 molar equiv of the Three Crown Ethers—**DB24C8**, **BPP34C10**, **1/5-DN38C10**—upon Complexation


	$2\text{-H}\cdot\text{PF}_6$ $\delta$	<b>DB24C8</b> $\delta$	complex $\delta$	$\Delta\delta$	<b>BPP34C10</b> $\delta$	complex $\delta$	$\Delta\delta$	<b>1/5-DN38C10</b> $\delta$	complex $\delta$	$\Delta\delta$
Ha	4.30		5.23	0.93		4.10	-0.2		4.22	-0.08
Hb	5.12		5.42	0.30		5.10	-0.02		5.06	-0.06
Hc	7.78		8.33	0.34		7.99	0.00		7.96	-0.03
Hd	8.53		8.00	-0.53		8.51	-0.02		8.49	-0.04
He	7.99		7.73	-0.11		7.77	-0.07		7.75	-0.09
Hf		6.79	6.56	-0.23						
Hg		6.79	6.20	-0.59						
Hh					6.62	6.48	-0.14			
Hi								7.63	7.59	-0.04
Hj								7.06	7.02	-0.04
Hk								6.34	6.34	-0.05

system at 25 °C. Further evidence for the formation of a 1:1 complex between  $2\text{-H}\cdot\text{PF}_6$  and **DB24C8** with a pseudorotaxane-like geometry has been obtained from the identification of intermolecular interactions—namely, between the protons on the crown ether's polyether chain and the benzylic methylene protons **Ha** and the **Hc** protons on the anthracenyl group. The fact that an NOE is observed between the benzylic methylene protons **Ha** and the *O*-methylene protons associated with the **DB24C8**'s polyether chain confirms the hypothesis that the benzylic group can penetrate deeply into the crown ether's cavity.

Since the equilibrium kinetics are slow on the  $^1\text{H}$  NMR time scale for an equimolar mixture of  $2\text{-H}\cdot\text{PF}_6$  and **DB24C8** in a mixture of  $\text{CDCl}_3$  and  $\text{CD}_3\text{CN}$  (6:1, v/v) at 25 °C, it is possible to determine the absolute concentration of the three species at equilibrium from integration of the spectrum, and hence, a single point determination<sup>13</sup> of the association constant can be made. In this manner, a  $K_a$  value of  $12\,600\text{ M}^{-1}$  was obtained for the 1:1 complex.

#### Mass Spectrometry: Formation of the Complex between $2\text{-H}\cdot\text{PF}_6$ and the Crown Ether **DB24C8** in the Gas Phase.

When LSI mass spectrometry was used to characterize the complex formed between  $2\text{-H}\cdot\text{PF}_6$  and the crown ether **DB24C8**, a peak for the  $[\text{M} - \text{PF}_6]^+$  ion was observed at  $m/z$  746 for  $[\text{DB24C8}\cdot\text{H}][\text{PF}_6]$ , confirming the 1:1 stoichiometry of the complex in the gas phase.

**X-ray Crystallography: Complex between  $2\text{-H}\cdot\text{PF}_6$  and the Crown Ether **BPP34C10** in the Solid State.** The X-ray analysis of the 1:2 complex formed between **BPP34C10** and  $2\text{-H}\cdot\text{PF}_6$  reveals (Figure 6) a characteristic geometry,<sup>7b</sup> namely the threading of a pair of  $\text{RR}'\text{NH}_2^+$  cations through the center of the **BPP34C10** macrocycle in a  $C_i$  symmetric arrangement. The 1:2 complex is stabilized by two pairs of  $[\text{N}^+ - \text{H}\cdots\text{O}]$  hydrogen bonds between the  $\text{NH}_2^+$  centers and the second and fourth oxygen atoms of each polyether loop. There are no secondary intracomplex  $[\text{C} - \text{H}\cdots\text{O}]$ ,  $[\text{C} - \text{H}\cdots\pi]$ , or  $\pi - \pi$  interactions. The conformation of the cation differs significantly from that observed in the complex between **DB24C8** and  $2\text{-H}\cdot\text{PF}_6$ , the  $\text{C} - \text{CH}_2 - \text{NH}_2^+ - \text{CH}_2 - \text{C}$  backbones being nonplanar with torsional twists about the two  $\text{C} - \text{N}$  bonds of  $104^\circ$  and

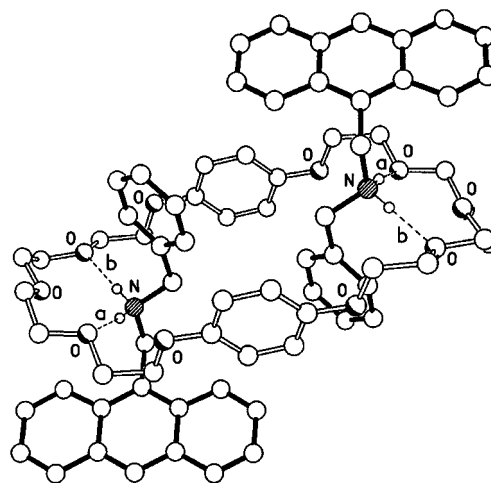


**Figure 6.** The superstructure in the crystal of the 1:2 complex formed between **BPP34C10** and  $2\text{-H}\cdot\text{PF}_6$ , showing the  $[\text{N}^+ - \text{H}\cdots\text{O}]$  hydrogen bonding. Hydrogen bonding geometries:  $[\text{N}^+ \cdots \text{O}]$ ,  $[\text{H}\cdots\text{O}]$  distances ( $\text{\AA}$ ),  $[\text{N}^+ - \text{H}\cdots\text{O}]$  angles (deg): (a) 2.99, 2.04, 168; (b) 2.96, 2.01, 169.

$177^\circ$ , the former twist being about the  $\text{N} - \text{C}$  bond toward the anthracene ring. The inclinations of the  $\text{C} - \text{N}$  bonds to their adjacent phenyl and anthracenyl rings are  $50^\circ$  and  $84^\circ$ , respectively. The intracomplex separation between the two  $\text{NH}_2^+$  centers is  $8.5\text{ \AA}$ . Investigation of the packing of the 1:2 complexes reveals the presence of an elegant two-dimensional  $\pi$ -stacked sheet with, in one direction, centrosymmetrically related pairs of anthracenyl rings being in a slightly offset parallel stacked geometry (mean interplanar separation of  $3.35\text{ \AA}$ ) and, in the other,  $\pi$ -stacked hydroquinone rings, also related by  $C_i$  symmetry (mean interplanar separation  $3.48\text{ \AA}$ , centroid-centroid distance  $4.09\text{ \AA}$ ).

**$^1\text{H}$  NMR Spectroscopy: Formation of the Complexes between  $2\text{-H}\cdot\text{PF}_6$  and the Crown Ether **BPP34C10** in Solution.** The addition of equimolar amounts of the crown ether **BPP34C10** to a solution of  $2\text{-H}\cdot\text{PF}_6$  in a mixture of  $\text{CDCl}_3$  and  $\text{CD}_3\text{CN}$  (6:1, v/v) at 25 °C produces shifts in the  $^1\text{H}$  NMR signals (Table 3). The observed changes in chemical shifts were not so pronounced as the ones recorded after addition of equimolar amounts of **DB24C8** to a solution of the ammonium

(13) Connors, K. A. *Binding Constants*, Wiley, New York, 1987.

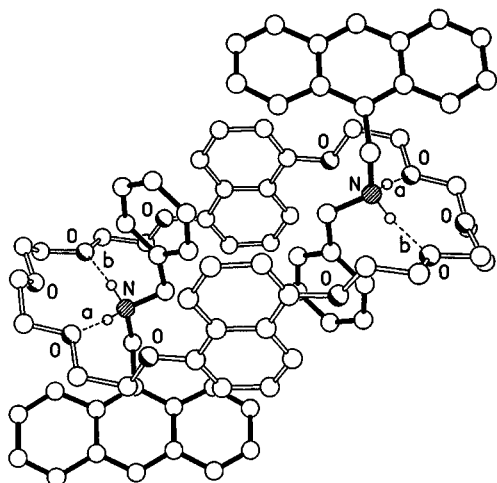


**Figure 7.** The superstructure in the crystal of the 1:2 complex formed **1/5-DN38C10** and **2-H·PF<sub>6</sub>**, showing the  $[N^+ \cdots H \cdots O]$  hydrogen bonding. Hydrogen bonding geometries:  $[N^+ \cdots O]$ ,  $[H \cdots O]$  distances (Å),  $[N^+ \cdots H \cdots O]$  angles (deg): (a) 3.02, 2.07, 168; (b) 2.98, 1.96, 161.

salt **2-H·PF<sub>6</sub>**. In the case of **BPP34C10**, downfield shifts are also observed for the methylene protons, particularly the benzylic methylene ones, and upfield shifts for the **Hc**, **Hd**, and **He** protons of the anthracenyl moiety in the ammonium cation. Upon complexation, the signals for the hydroquinone rings of the crown ether are shifted upfield. The three distinct sets of resonances for the free components and for the complex are not observed as in the case of the complex with **DB24C8**, presumably because the equilibrium between the complexed and the uncomplexed species is now fast on the <sup>1</sup>H NMR time scale at room temperature. Thus, the chemical shifts listed in Table 3 are the time-averaged signals for the complexed and uncomplexed species involving **BPP34C10** with **2-H·PF<sub>6</sub>**. The **2-H·PF<sub>6</sub>** salt has a very low solubility in  $CD_2Cl_2$ , but it can be dissolved in the presence of an equimolar amount of **BPP34C10**. Additionally, it is interesting to note that the <sup>1</sup>H NMR spectrum, obtained after filtration of a suspension of an excess of **2-H·PF<sub>6</sub>** in  $CD_2Cl_2$  containing **BPP34C10**, showed a stoichiometry associated with a 1:2 complex,  $[BPP34C10 \cdot (2-H \cdot PF_6)_2]$ .

#### Mass Spectrometry: Formation of the Complex between **2-H·PF<sub>6</sub>** and the Crown Ether **BPP34C10** in the Gas Phase.

When LSI mass spectrometry was used to characterize the complex formed between **2-H·PF<sub>6</sub>** and **BPP34C10**, a peak for the  $[M - PF_6]^+$  ion was observed at  $m/z$  1277 for  $[BPP34C10 \cdot (2-H)_2][PF_6]$ , confirming that the 1:2 stoichiometry also exists in the gas phase.

#### X-ray Crystallography: Complex between **2-H·PF<sub>6</sub>** and the Crown Ether **1/5-DN38C10** in the Solid State.

The solid state structure of the 1:2 complex formed between **1/5-DN38C10** and **2-H·PF<sub>6</sub>** shows (Figure 7) the two cations to be threaded through the center of the macrocycle, adopting an overall geometry similar to that observed for the 1:2 complex involving **BPP34C10**. The superstructure once again has crystallographic  $C_i$  symmetry and is stabilized by a combination of  $[N^+ \cdots H \cdots O]$  and  $[C-H \cdots \pi]$  hydrogen bonding interactions. The former are between the  $NH_2^+$  centers and the second and fourth oxygen atoms of the polyether loops, whereas the latter is from a naphthyl hydrogen atom H-2 and one of the outer six-membered rings of an adjacent anthracenyl ring system—the  $[H \cdots \pi]$  distances and  $[C-H \cdots \pi]$  angles are 2.92 Å and 143°, respectively. The  $C-CH_2-NH_2^+-CH_2-C$  backbones of each cation are again nonplanar with  $C-N$  torsional angles of 87° (toward the anthracenyl group) and 77° (toward the phenyl group). The  $C-N$  bond adjacent to the anthracenyl ring system is inclined

by 84° to the ring plane, whereas that adjacent to the phenyl ring is inclined by 33° and 47°—there being two alternate orientations for the phenyl ring in the structure. The intramolecular  $N \cdots N$  separation is 9.1 Å. The mode of packing of the 1:2 complexes differs from that observed for the **BPP34C10** analog in that the  $\pi-\pi$  stacking is only unidirectional, involving the 1,5-dioxynaphthalene ring systems of the **1/5-DN38C10** macrocycles. The naphtho rings are parallel with an interplanar separation of 3.38 Å, but offset such that one of the hydrogen atoms of the attached  $OCH_2$  group in one molecule is directed into the center of one of the six-membered rings of the 1,5-dioxynaphthalene ring system of the next complex. The  $[H \cdots \pi]$  distance is 2.64 Å and the associated  $[C-H \cdots \pi]$  angle is 149°.

#### <sup>1</sup>H NMR Spectroscopy: Formation of the Complexes between **2-H·PF<sub>6</sub>** and the Crown Ether **1/5-DN38C10** in Solution.

The addition of equimolar amounts of the crown ether **1/5-DN38C10** to a solution of **2-H·PF<sub>6</sub>** in a mixture of  $CDCl_3$  and  $CD_3CN$  (6:1, v/v) at 25 °C produces shifts in the <sup>1</sup>H NMR signals (Table 3). The observed changes in chemical shifts were not so pronounced as the ones recorded after addition of equimolar amounts of **DB24C8** to a solution of the ammonium salt **2-H·PF<sub>6</sub>**. In the case of the macrocycle **1/5-DN38C10**, downfield shifts are also observed for the methylene protons, particularly the benzylic methylene ones, and upfield shifts for the **Hc**, **Hd**, and **He** protons of the anthracenyl group in the ammonium cation. Upon complexation, the signals for the 1,5-dioxynaphthalene rings of the crown ether are shifted upfield. The three distinct sets of resonances for the free components and for the complex are not observed (*cf.*, the complex with **DB24C8**), presumably because the equilibrium between the complexed and the uncomplexed species is fast on the <sup>1</sup>H NMR time scale at room temperature. Thus, the chemical shifts listed in Table 3 are the time-averaged signals for the complexed and uncomplexed species involving **1/5-DN38C10** and **2-H·PF<sub>6</sub>**. It was not possible to perform complexation experiments in  $CD_2Cl_2$  with **1/5-DN38C10** because of the insolubility of this crown ether in this solvent. When  $CDCl_3$  was used as the solvent, in which the crown ether is indeed soluble, it did not extract the salt **2-H·PF<sub>6</sub>**. In the <sup>1</sup>H NMR spectrum, only signals for the uncomplexed crown ether are present. Similar results were obtained when attempting to use **BPP34C10** to extract **2-H·PF<sub>6</sub>** into  $CDCl_3$ .

#### Mass Spectrometry: Formation of the Complex between **2-H·PF<sub>6</sub>** and the Crown Ether **1/5-DN38C10** in the Gas Phase.

When LSI mass spectrometry was used to characterize the complex formed between **2-H·PF<sub>6</sub>** and **1/5-DN38C10**, a peak for the  $[M - PF_6]^+$  ion was observed at  $m/z$  1377 for  $[1/5-DN38C10 \cdot (2-H)_2][PF_6]$ , confirming that the 1:2 stoichiometry also exists in the gas phase.

### Photophysical Processes in the Complexes

#### Complexes with Dibenzocrown Ethers **DB18C6-DB30C10**.

The complexes of **1-H·PF<sub>6</sub>** and **2-H·PF<sub>6</sub>** with the crown ethers **DB18C6-DB30C10** exhibit very similar properties in their UV/vis spectra. The absorption spectra of the  $CH_2Cl_2$  solutions, containing equimolar amounts of protonated amines and crown ethers ( $1.0 \times 10^{-4}$  M), are very close to that of the sums of the separate components.

Upon excitation at 276 nm (where most of the light is absorbed by the crown ether moiety (Figure 2)), the crown ether **DB24C8** fluorescence ( $\lambda_{max} = 312$  nm) is almost completely quenched and that of the protonated amine ( $\lambda_{max} = 423$  nm) is much higher than that expected for the separate components (Figure 8). This means that the fluorescent excited state of the crown ether is deactivated by energy transfer to the lower lying

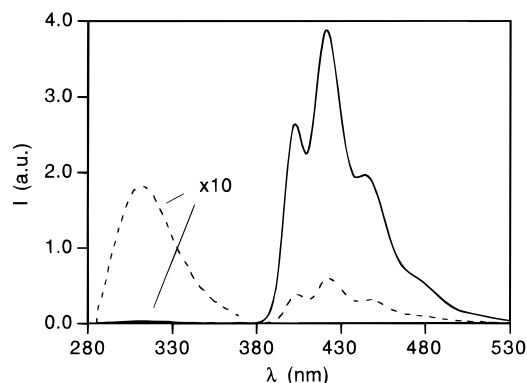


**Figure 8.** Fluorescence spectra of a  $\text{CH}_2\text{Cl}_2$  solution containing  $1 \times 10^{-4}$  M  $2\text{-H}\cdot\text{PF}_6$  and **DB24C8** (full lines) compared with the sum of the spectra of the separated components (dashed lines). The excitation wavelength is 276 nm.

fluorescent excited state of the anthracene moiety of the protonated amine (Figure 9a). Upon excitation in the absorption bands of the anthracene moiety, a fluorescence band is observed which matches closely that of the protonated amine alone. A comparison between the absorption and excitation spectra in the whole spectral region shows that energy transfer from the crown ether to the anthracene moiety is 100% efficient in the complex. At 77 K, the phosphorescence band of the crown ether is not present in the complex.

**Complexes with 1/5-DN38C10.** For the complexes of  $1\text{-H}\cdot\text{PF}_6$  and  $2\text{-H}\cdot\text{PF}_6$  with the crown ether **1/5-DN38C10**, the absorption spectra are very close to the sum of the spectra of the separate components. In the fluorescence spectrum of a  $\text{CH}_2\text{Cl}_2$  solution containing equimolar amounts ( $1.0 \times 10^{-4}$  M) of  $1\text{-H}\cdot\text{PF}_6$  or  $2\text{-H}\cdot\text{PF}_6$  and **1/5-DN38C10**, upon excitation at 296 nm (where most of the light is absorbed by the crown ether moiety, Figure 2), the intensity of the crown ether band ( $\lambda_{\text{max}} = 345$  nm) is smaller and that of the protonated amine ( $\lambda_{\text{max}} = 432$  nm) is higher than that expected for the separate components. At first sight, this would suggest that the fluorescent excited state of the crown ether is deactivated by energy transfer to the lower lying fluorescent excited state of the anthracene moiety of the protonated amine. Closer scrutiny of the results, however, shows that the observed effect is related to the fraction of unassociated species. Since the emission spectrum of **1/5-DN38C10** overlaps the absorption spectrum of the anthracene chromophoric unit of the protonated amine, the light emitted by the fraction of free crown ether molecules is absorbed by the fraction of free  $2\text{-H}\cdot\text{PF}_6$  species, causing a trivial sensitization effect. When such an effect is taken into account, it is clear that, in the complexes, the fluorescence of the crown ether moiety is completely quenched by the anthracene unit, without causing any sensitized emission from the latter. We have also found that, upon excitation at 361 nm (where only the anthracene chromophoric unit absorbs light, Figure 2), the intensity of the anthracene is quenched by the formation of the complex with the crown ether. These results indicate that, in the complex involving **1/5-DN38C10**, both the fluorescence of the crown ether and the fluorescence of the protonated amine are completely quenched. This is not surprising if we consider the energy ordering of the excited states of the two chromophoric units (Figure 9b). In these complexes, the anthracene fluorescence does not survive because the triplet state of the dioxynaphthalene moiety lies below the  $S_1$  excited state of the anthracene unit. At 77 K, one can see that the phosphorescence band of the crown ether is also quenched, presumably by energy transfer to the lower lying triplet excited state of the anthracene unit (which is not emissive).

**Complexes with 2/3-DN30C10.** For the complexes of  $1\text{-H}\cdot\text{PF}_6$  and  $2\text{-H}\cdot\text{PF}_6$  with the crown ether **2/3-DN30C10**, the absorption spectrum of the complex is noticeably different from the sum of the spectra of separate components (Figure 10). Particularly worth noting is the presence of an absorption tail above 400 nm, not present in the spectrum of the separate compounds, which suggests the presence of an energy level arising from the interaction between the two components. Such an interaction is likely to be charge-transfer in nature since the 2,3-dinaphtho chromophoric unit of the crown ether is an electron donor (its oxidation occurs at +1.39 V in MeCN)<sup>11a</sup> and the anthracene unit of the protonated amine can play the role of electron acceptor (reduction potential, -1.97 V for 9-methylanthracene in MeCN).<sup>11a</sup>

In the fluorescence spectrum of a  $\text{CH}_2\text{Cl}_2$  solution containing equimolar amounts ( $1.0 \times 10^{-4}$  M) of  $2\text{-H}\cdot\text{PF}_6$  and **2/3DN30C10** upon excitation at 290 nm (where most of the light is absorbed by the crown ether moiety), the intensity of the crown ether band ( $\lambda_{\text{max}} = 342$  nm) is extremely weak and a new, broad band with  $\lambda_{\text{max}} = 435$  nm appears (Figure 11). The broad band is also observed when excitation is performed at 361 nm, where only the anthracene chromophoric unit absorbs light. When excitation is performed at 290 nm (where light is mostly absorbed by the 2,3-dinaphtho chromophoric unit of the crown ether), the experimental spectrum matches that expected in the case of 100% energy-transfer efficiency in the complex from the fluorescent excited state of the 2,3-dinaphtho crown ether to the state responsible for the broad band with  $\lambda_{\text{max}} = 435$  nm.

These results show that, in the complex of **2/3-DN30C10**, both the fluorescent excited state of the crown ether and the fluorescent excited state of the protonated amine are completely quenched by a lower energy excited state resulting from the interaction of the two chromophoric units. Such an excited state, indicated by CT in Figure 9c, is responsible for the broad emission band with  $\lambda_{\text{max}} = 435$  nm and most likely also for the low-energy tail of the absorption spectrum (*vide supra*). Apparently, in the complexes involving **2/3-DN30C10**, the interaction between the anthracene moiety and the aromatic units of the crown ether is relatively stronger than it is for the other complexes. It should also be noted that the state responsible for the broad emission is not (completely) quenched by the lower lying triplet excited state of the crown ether (Figure 9c). This is consistent with the charge-transfer nature of the emitting level, a situation which could imply a considerable reorganizational barrier for deactivation to the localized crown ether level.

**Complexation Reversibility by Deprotonation and Reprotonation.**<sup>14</sup> Experiments, monitored by  $^1\text{H}$  NMR spectroscopy, were performed in order to demonstrate the reversibility of the complexation process occurring between **DB24C8** and  $2\text{-H}\cdot\text{PF}_6$  by deprotonating and reprotonating the  $\text{RR}'\text{NH}_2^+$  ion. An equimolar solution of **DB24C8** and  $2\text{-H}\cdot\text{PF}_6$  was prepared in a mixture of  $\text{CDCl}_3$  and  $\text{CD}_3\text{CN}$  (6:1, v/v) at 25 °C (Figure 12a), and then a slight molar excess of quinuclidine was added to the solution to deprotonate the  $\text{NH}_2^+$  center (Figure 12b). Finally,  $\text{CF}_3\text{COOH}$  was added to reprotonate the amine (Figure 12c). The same procedure was followed in the fluorescence experiment, but using a  $1 \times 10^{-4}$  M equimolar  $\text{CH}_2\text{Cl}_2$  solution of **DB24C8** and  $2\text{-H}\cdot\text{PF}_6$ .

Upon inspection of the three  $^1\text{H}$  NMR spectra (Figure 12a–c), it is clear that, initially, we observed the 1:1 complex, which then disassembles into the two components on adding the base. Upon addition of  $\text{CF}_3\text{COOH}$ , all signals for the complex are

(14) For a recent example of how pH can effect the topology of supramolecular systems, see: Shimizu, T.; Kogiso, M.; Masuda, M. *J. Am. Chem. Soc.* **1997**, *119*, 6209–6210 and references cited therein.

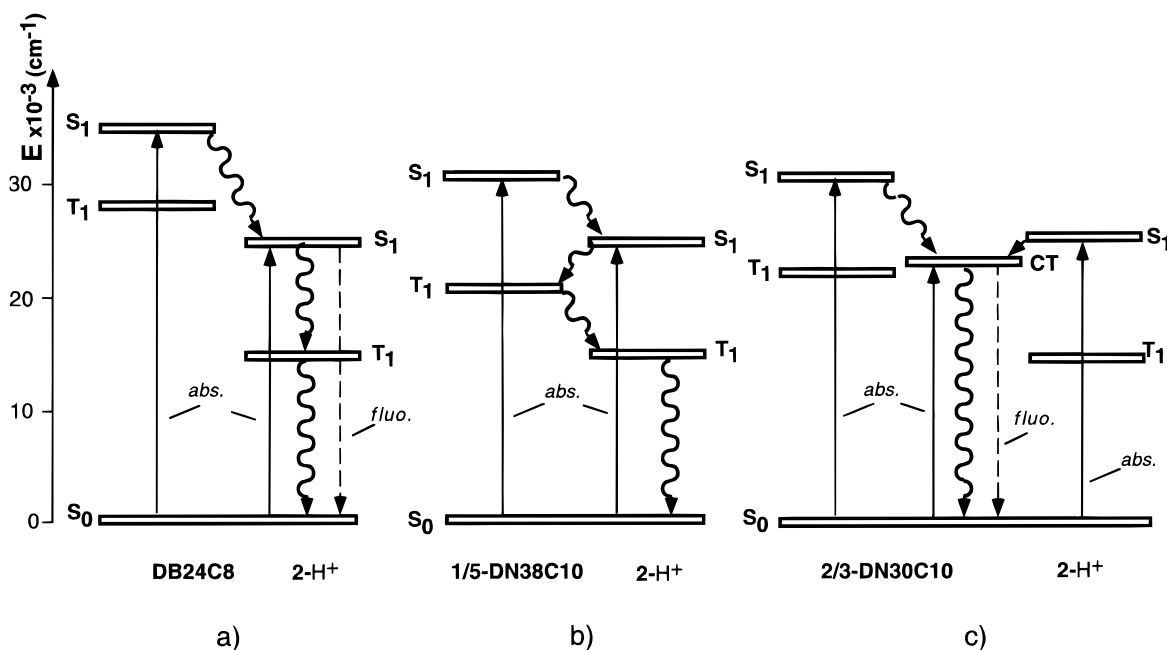


**Figure 9.** Schematic energy-level diagrams for the complexes of  $1\text{-H}\cdot\text{PF}_6$  or  $2\text{-H}\cdot\text{PF}_6$  with (a) 1,2-dibenzocrown ethers **DB18C6-DB30C10**, (b) 1,5-dinaphtho crown ether **1/5-DN38C10**, and (c) 2,3-dinaphtho crown ether **2/3-DN30C10**.

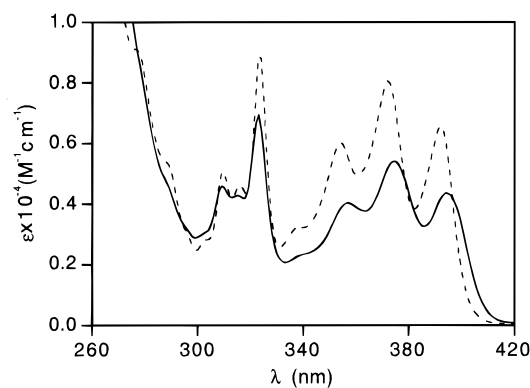


**Figure 10.** Absorption spectra of a  $\text{CH}_2\text{Cl}_2$  solution containing  $1 \times 10^{-4}$  M  $2\text{-H}\cdot\text{PF}_6$  and **2/3-DN30C10** (full lines) compared with the sum of the spectra of the separated components (dashed lines).

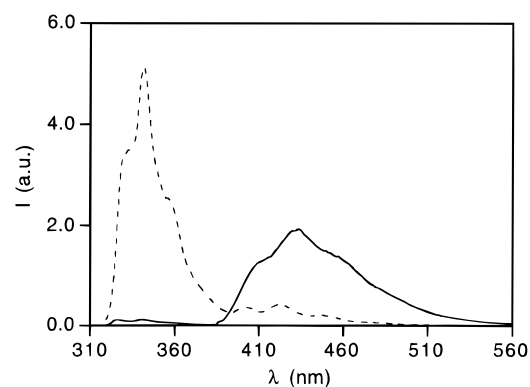


**Figure 11.** Fluorescence spectra of a solution of a  $\text{CH}_2\text{Cl}_2$  solution containing  $1 \times 10^{-4}$  M  $2\text{-H}\cdot\text{PF}_6$  and **2/3-DN30C10** (full lines) compared with the sum of the spectra of the separated components (dashed lines). The excitation wavelength is 290 nm.

then observed once again in the  $^1\text{H}$  NMR spectrum, confirming the reversibility of the process. It is interesting to note that the resonances for  $\text{Ha}_{\text{uc}}$  and  $\text{Hb}_{\text{uc}}$ , after reprotonation by addition of  $\text{CF}_3\text{COOH}$ , are slightly shifted with respect to the resonances for the same protons in  $2\text{-H}\cdot\text{PF}_6$  (Figure 12a). Presumably, this effect is a result of the presence in solution of both the

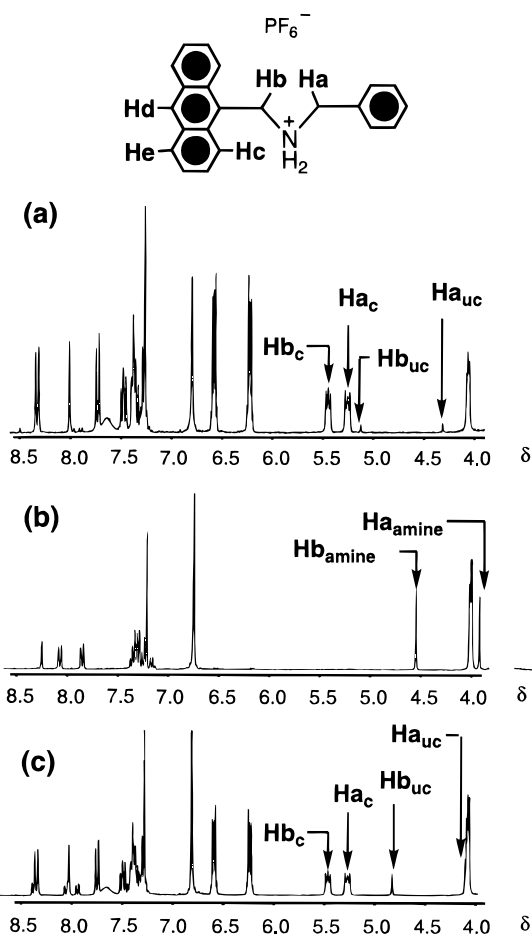


**Figure 12.**  $^1\text{H}$  NMR (300 MHz,  $\text{CDCl}_3/\text{MeCN}$ , 6:1) spectra of (a) a 1:1 mixture of  $2\text{-H}\cdot\text{PF}_6$  and **DB24C8**, of (b) a 1:1 mixture of  $2\text{-H}\cdot\text{PF}_6$  and **DB24C8** after addition of quinuclidine, and of (c) a 1:1 mixture of  $2\text{-H}\cdot\text{PF}_6$  and **DB24C8** after addition of quinuclidine and subsequently  $\text{CF}_3\text{COOH}$ .

$\text{CF}_3\text{COO}^-$  and the  $\text{PF}_6^-$  counterions. The solvation of the  $\text{NH}_2^+$  center, after having been complexed by **DB24C8**, results in no significant shift for the resonance of the  $\text{Ha}_{\text{c}}$  and  $\text{Hb}_{\text{c}}$ , as shown



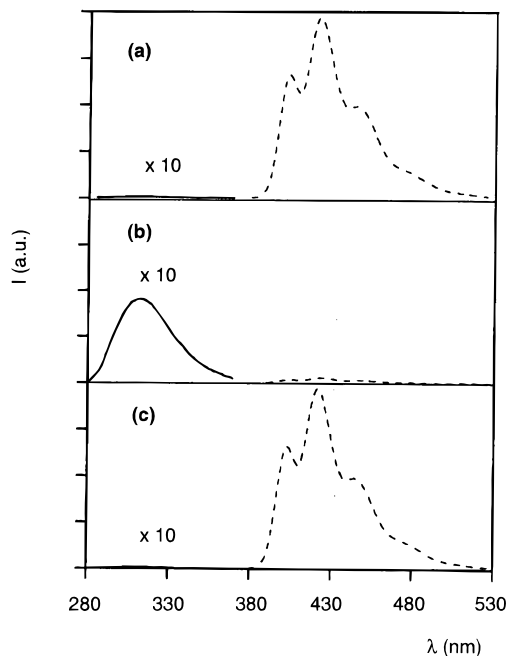


**Figure 13.** Fluorescence spectra ( $\lambda_{\text{exc}} = 276$  nm,  $\text{CH}_2\text{Cl}_2$  solution) of (a) a 1:1 mixture of **2-H**· $\text{PF}_6$  and **DB24C8**, (b) a 1:1 mixture of **2-H**· $\text{PF}_6$  and **DB24C8**, after addition of quinuclidine, and (c) a 1:1 mixture of **2-H**· $\text{PF}_6$  and **DB24C8**, after addition of quinuclidine and subsequently  $\text{CF}_3\text{COOH}$ .

in Figure 12a,c. However, the uncomplexed  $\text{NH}_2^+$  center experiences the effect of these different counterions, and so the chemical shifts alter considerably.

The reversibility of the complexation process is clearly confirmed by the fluorescence experiment (Figure 13). The emission spectrum ( $\lambda_{\text{exc}} = 276$  nm, where light is mostly absorbed by the crown ether moiety) of an equimolar solution of **DB24C8** and **2-H**· $\text{PF}_6$ , in which the formation of a complex is demonstrated by the occurrence of energy transfer from the excited states of the crown to the fluorescent excited state of the anthracene moiety, is displayed in Figure 13a. The disassembling of the complex by adding the base is shown by the complete recovery of the fluorescence band of the dialkoxybenzene units of **DB24C8** (Figure 13b). Upon addition of acid, the spectral changes are almost quantitatively reversed (Figure 13c).

## Conclusions

$\text{RR}'\text{NH}_2^+$  ions containing an anthracene moiety give rise to complexes with crown ethers containing dibenzo, *i.e.*, dialkoxybenzene (**DB**), or dinaphtho, *i.e.*, dialkoxynaphthalene (**DN**) units. For some of the complexes of **2-H**· $\text{PF}_6$ , a pseudorotaxane structure is demonstrated by  $^1\text{H}$  NMR spectroscopy, X-ray crystallography, mass spectrometry, and spectrofluorimetry. The association constants decrease according to the counterion series,  $\text{PF}_6^- > \text{CF}_3\text{SO}_3^- > \text{CF}_3\text{COO}^-$ . In the complexes, relatively weak electronic interactions take place between the chromophoric units present in the two components. In all cases, the fluorescence of the dialkoxybenzene or dialkoxynaphthalene units of the crown is completely quenched. In the complexes of the **DB18C6**, **DB24C8**, and **DB30C10** macrocycles, the quenching of the fluorescence of the dialkoxybenzene units is accompanied by a parallel sensitization of the anthracene fluorescence. In the complexes of **1/5-DN38C10**, the anthracene fluorescence is also completely quenched, most likely by energy transfer from the  $\text{S}_1$  excited state of the anthracene moiety to the lower lying triplet excited state of the dialkoxynaphthalene

unit. In the complexes of **2/3DN30C10**, the interaction between the anthracene moiety and the aromatic units of the crown ether is relatively strong, as indicated by perturbation of the absorption bands. The fluorescence of both the naphtho and the anthracene chromophoric units is completely quenched, and a new, broad luminescence band with  $\lambda_{\text{max}} = 435$  nm, assigned to a charge-transfer level, dominates the emission spectrum.

These results extend the notion<sup>9,15</sup> that electronic interactions, sufficiently strong to change the luminescence properties and to cause intercomponent energy- and/or electron-transfer processes, can be driven by association processes based on hydrogen bonds. These observations will help in the design of new families of supramolecular systems capable of exploiting the energy and/or information content of light.

Finally, the reversible on–off switching of complex formation of the  $\text{RR}'\text{NH}_2^+$  ion with **DB24C8** has been investigated. Upon addition of a suitable base, deprotonation of the  $\text{NH}_2^+$  center takes place, thus causing the dethreading of the **DB24C8** macrocycle. Addition of a suitable acid reprotonates the amine and the original 1:1 pseudorotaxane-like inclusion complex is regenerated, rendering the cycle reversible. This process can be monitored by  $^1\text{H}$  NMR and fluorescence spectroscopy.

The next logical step in the search for nanoscale switchable systems is the construction of a discrete molecular species—a [2]rotaxane<sup>16</sup> comprising two nondegenerate stations<sup>17</sup> in its dumbbell-shaped component. Investigations in this direction are underway.<sup>18</sup>

## Experimental Section

**General Methods.** The routine procedures have been described elsewhere.<sup>19</sup> Chemicals were purchased from Aldrich and used without further purification. The crown ethers **DB18C6**, **DB24C8**, and **DB30C10** and 9-[(methylamino)methyl]anthracene (**1**) are commercial products. **BPP34C10**,<sup>20</sup> **2/3-DN30C10**,<sup>21</sup> and **1/5-DN38C10**<sup>22</sup> were prepared, according to literature procedures. The absorption and emission experiments were carried out in  $\text{CH}_2\text{Cl}_2$  solution at 298 K, except for the phosphorescence spectra which were performed in a rigid

(15) (a) Fages, F.; Desvergne, J.-P.; Bouas-Laurent, H.; Marsau, P.; Lehn, J.-M.; Kotzyba-Hilbert, F.; Albrecht-Gary, A.-M.; Al-Joubbeh, M. *J. Am. Chem. Soc.* **1989**, *111*, 8672–8680. (b) Desvergne, J.-P.; Fages, F.; Bouas-Laurent, H.; Marsau, P. *Pure Appl. Chem.* **1992**, *64*, 1231–1238. (c) Balzani, V.; Ballardini, R.; Gandolfi, M. T.; Prodi, L. In *Frontiers in Supramolecular Organic Chemistry and Photochemistry*; Schneider, H.-J., Dürr, H., Eds.; VCH: Weinheim, 1991; pp 371–391. (d) Ballardini, R.; Balzani, V.; Credi, A.; Gandolfi, M. T.; Kotzyba-Hilbert, F.; Lehn, J.-M.; Prodi, L. *J. Am. Chem. Soc.* **1994**, *116*, 5741–5746.

(16) Schill, G. *Catenanes, Rotaxanes and Knots*; Academic Press: New York, 1971.

(17) (a) Ashton, P. R.; Bissell, R. A.; Spencer, N.; Stoddart, J. F.; Tolley, M. S. *Synlett* **1992**, 914–918. (b) Ashton, P. R.; Bissell, R. A.; Górski, R.; Philp, D.; Spencer, N.; Stoddart, J. F.; Tolley, M. S. *Synlett* **1992**, 919–922. (c) Ashton, P. R.; Bissell, R. A.; Spencer, N.; Stoddart, J. F.; Tolley, M. S. *Synlett* **1992**, 923–926. (d) Bissell, R. A.; Córdova, E.; Kaifer, A. E.; Stoddart, J. F. *Nature (London)* **1994**, *369*, 133–137. (e) Amabilino, D. B.; Ashton, P. R.; Boyd, S. E.; Gómez-López, M.; Hayes, W.; Stoddart, J. F. *J. Org. Chem.* **1997**, *62*, 3062–3075. (f) Anelli, P. L.; Asakawa, M.; Ashton, P. R.; Bissell, R. A.; Clavier, G.; Górski, R.; Kaifer, A. E.; Langford, S. J.; Matternsteig, G.; Menzer, S.; Philp, D.; Slawin, A. M. Z.; Spencer, N.; Stoddart, J. F.; Tolley, M. S.; Williams, D. J. *Chem. Eur. J.* **1997**, *3*, 1113–1135.

(18) Martínez-Díaz, M.-V.; Spencer, N.; Stoddart, J. F. *Angew. Chem., Int. Ed. Engl.* **1997**, *36*, 1904–1907.

(19) Asakawa, M.; Ashton, P. R.; Brown, C. L.; Fyfe, M. C. T.; Menzer, S.; Pasini, D.; Scheuer, C.; Spencer, N.; Stoddart, J. F.; White, A. J. P.; Williams, D. J. *Chem. Eur. J.* **1997**, *3*, 1136–1150.

(20) Helgeson, R. C.; Tarnowski, T. L.; Timko, J. M.; Cram, D. J. *J. Am. Chem. Soc.* **1977**, *99*, 6411–6418.

(21) Colquhoun, H. M.; Goodings, E. P.; Maud, J. M.; Stoddart, J. F.; Wolstenholme, J. B.; Williams, D. J. *J. Chem. Soc., Perkin Trans. 2* **1985**, 607–624.

(22) Ashton, P. R.; Ballardini, R.; Balzani, V.; Credi, A.; Gandolfi, M. T.; Menzer, S.; Pérez-García, L.; Prodi, L.; Stoddart, J. F.; Venturi, M.; White A. J. P.; Williams, D. J. *J. Am. Chem. Soc.* **1995**, *117*, 11171–11197.

**Table 4.** Crystal Data, Data Collection and Refinement Parameters<sup>a</sup>

data	[DB24C8·2-H][PF <sub>6</sub> ]	[BPP34C10·(2-H) <sub>2</sub> ][PF <sub>6</sub> ] <sub>2</sub>	[1/5-DN38C10·(2-H) <sub>2</sub> ][PF <sub>6</sub> ] <sub>2</sub>
formula	C <sub>46</sub> H <sub>52</sub> N <sub>2</sub> O <sub>8</sub> ·PF <sub>6</sub>	C <sub>72</sub> H <sub>80</sub> N <sub>2</sub> O <sub>10</sub> ·2PF <sub>6</sub>	C <sub>80</sub> H <sub>84</sub> N <sub>2</sub> O <sub>10</sub> ·2PF <sub>6</sub>
solvent			MeCN·CHCl <sub>3</sub>
formula weight	891.9	1423.3	1844.3
color, habit	colorless prisms	colorless prisms	colorless prisms
crystal size/mm	0.73 × 0.66 × 0.60	0.63 × 0.33 × 0.30	0.46 × 0.33 × 0.27
lattice type	triclinic	triclinic	triclinic
space group	<i>P</i> $\bar{1}$	<i>P</i> $\bar{1}$	<i>P</i> $\bar{1}$
cell dimensions			
<i>a</i> /Å	12.622(2)	11.023(1)	11.335(2)
<i>b</i> /Å	17.099(2)	12.594(1)	13.126(2)
<i>c</i> /Å	21.970(5)	14.259(2)	17.640(3)
$\alpha$ /deg	94.36(2)	74.27(1)	70.96(1)
$\beta$ /deg	102.53(2)	72.63(1)	73.03(1)
$\gamma$ /deg	103.16(1)	64.17(1)	66.50(1)
<i>V</i> /Å <sup>3</sup>	4468(2)	1677.4(4)	2235.4(6)
<i>Z</i>	4 <sup>b</sup>	1 <sup>c</sup>	1 <sup>c</sup>
<i>D</i> <sub>c</sub> /g cm <sup>-3</sup>	1.326	1.409	1.370
<i>F</i> (000)	1872	744	956
radiation used	Mo K $\alpha$	Mo K $\alpha$	Cu K $\alpha$
$\mu$ /mm <sup>-1</sup>	0.14	0.16	2.81
$\theta$ range/deg	1.8–22.5	1.8–22.5	2.7–60.0
no. of unique reflections			
measured	11689	4390	6570
observed, $ F_o  > 4\sigma( F_o )$	5173	2984	4377
no. of variables	1120	461	558
<i>R</i> <sub>1</sub> <sup>d</sup>	0.085	0.047	0.081
<i>wR</i> <sub>2</sub> <sup>e</sup>	0.198	0.109	0.213
weighting factors <i>a</i> , <i>b</i> <sup>f</sup>	0.096, 4.822	0.048, 0.531	0.130, 2.460
largest difference peak, hole/eÅ <sup>-3</sup>	0.77, -0.25	0.20, -0.17	0.41, -0.41

<sup>a</sup> Details in common: graphite monochromated radiation,  $\omega$ -scans, Siemens P4 diffractometer, refinement based on  $F^2$ , 293 K. <sup>b</sup> There are two crystallographically independent molecules in the asymmetric unit. <sup>c</sup> The molecule has crystallographic *C*<sub>1</sub> symmetry. <sup>d</sup>  $R_1 = \sum ||F_o| - |F_c|| / \sum |F_o|$ . <sup>e</sup>  $wR_2 = \{ \sum [w(F_o^2 - F_c^2)^2] / \sum [w(F_o^2)^2] \}^{1/2}$ . <sup>f</sup>  $w^{-1} = \sigma^2(F_o^2) + (aP)^2 + bP$ .

matrix at 77 K. Equipment for photophysical measurements and procedures have been described previously.<sup>12a</sup>

**Spectrofluorimetric Determination of Association Constants.** The association constants of the complexes can be estimated by analyzing the decrease in fluorescence intensity of the crown ether as a function of the 1-H·PF<sub>6</sub> or 2-H·PF<sub>6</sub> concentration. The intensity, read at the maximum of the crown ether band, was corrected in order to take into account inner filter and instrumental effects,<sup>23</sup> and then it was fitted to  $I_{corr} = \phi_{cr} C_{cr}$  where  $C_{cr}$  is the concentration of uncomplexed crown and  $\phi_{cr}$  is the proportionality constant between the corrected emission intensity (in arbitrary units) and the concentration of the uncomplexed crown ether.  $C_{cr}$  satisfies eq 1, where  $C_{cr}^o$  is the total concentration of the crown ether and  $C_{com}$  the complex concentration.

$$C_{cr} = C_{cr}^o - C_{com} \quad (1)$$

$C_{com}$  satisfies the usual 1:1 binding expression in eq 2 where  $C_{am}^o$  is the total concentration of added ammonium ion.

$$C_{com}^2 - (C_{cr}^o + C_{am}^o + 1/K_a)C_{com} + C_{am}^o C_{cr}^o = 0 \quad (2)$$

Equilibrium constants  $K_a$  were then obtained by simulation of the data with both  $K_a$  and  $\phi_{cr}$  as adjustable parameters and minimizing the sum of squares of residuals.

**(9-Anthracenyl)methylbenzylammonium Hexafluorophosphate (2-H·PF<sub>6</sub>).** A solution of 9-anthracenealdehyde (4.95 g, 0.024 mol) and benzylamine (2.59 g, 0.024 mol) in PhMe (150 mL) was heated under reflux with stirring in a Dean-Stark apparatus for 14 h. After the reaction mixture had been cooled down to room temperature, the solvent was removed *in vacuo* to give the imine as brownish solid. The solid was dissolved in hot MeOH (100 mL), followed by portionwise addition of NaBH<sub>4</sub> (2.73 g, 0.072 mol) and heating under reflux with stirring for 10 h. The reaction mixture was then allowed to cool down to room temperature, and concentrated HCl was added (pH < 2). After evaporation of the solvent, the residue was suspended in H<sub>2</sub>O (50 mL) and extracted with CH<sub>2</sub>Cl<sub>2</sub> (4 × 50 mL). The combined extracts were washed with 5% aqueous NaHCO<sub>3</sub> (2 × 60

mL) and H<sub>2</sub>O (50 mL) and then dried (MgSO<sub>4</sub>). Removal of the solvent *in vacuo* and purification by silica gel column chromatography (eluent: MeOH/CH<sub>2</sub>Cl<sub>2</sub>, 1:30) afforded the amine **2** (5.74 g, 80%) as a pale yellow solid with mp > 48 °C dec. The amine **2** (2.00 g, 6.7 mmol) was dissolved in MeOH (50 mL). Concentrated HCl was added dropwise (pH < 2), and the reaction mixture was stirred for a further 2 h. Evaporation of the solvent and recrystallization of the crude product from a mixture of MeOH/Et<sub>2</sub>O afforded the pure ammonium hydrochloride salt 2-H·Cl (770 mg, 34%) as a pale yellow solid with mp > 204 °C dec. The hydrochloride salt (770 mg, 2.3 mmol) was then suspended in Me<sub>2</sub>CO (30 mL), and an aqueous solution of NH<sub>4</sub>-PF<sub>6</sub> (752 mg, 4.6 mmol) was added. The reaction mixture was stirred for 30 min. Evaporation of the solvent afforded pale yellow crystals of the ammonium hexafluorophosphate salt 2-H·PF<sub>6</sub> which were filtered off, washed with H<sub>2</sub>O, and air-dried (1.00 g, 98%): mp > 187 °C (dec.); <sup>1</sup>H NMR (300 MHz, CD<sub>3</sub>COCD<sub>3</sub>)  $\delta$  4.25 (s, 2H; CH<sub>2</sub>N), 5.02 (s, 2H; CH<sub>2</sub>N), 7.35 (s, 5H; aromatic CH), 7.35–7.48 (m, 4H; anthracene H-2, H-4, H-5, H-7), 7.80 (d,  $J_{2,3} = J_{7,8} = 9.0$  Hz, 2H; anthracene H-2, H-8), 7.95 (d,  $J_{3,4} = J_{5,6} = 9.0$  Hz, 2H; anthracene H-4, H-5), 8.49 (s, 1H; anthracene H-10); <sup>13</sup>C NMR (75.5 MHz, CD<sub>3</sub>-COCD<sub>3</sub>)  $\delta$  44.3, 53.3, 124.1, 126.4, 128.3, 130.0, 130.27, 130.6, 131.3, 131.8, 132.2, 206.1; MS (LSI) *m/z* 298 [M - PF<sub>6</sub>]<sup>+</sup>, 207 [M - PF<sub>6</sub> - C<sub>6</sub>H<sub>5</sub>CH<sub>2</sub>]<sup>+</sup>, 191 [M - PF<sub>6</sub> - C<sub>6</sub>H<sub>5</sub>CH<sub>2</sub>NH]<sup>+</sup>. Anal. Calcd for C<sub>22</sub>H<sub>20</sub>NPF<sub>6</sub>: C, 59.6; H, 4.55; N, 3.16. Found C, 59.8; H, 4.42; N, 3.02.

**X-ray Crystallography.** Single crystals, suitable for X-ray crystallographic analysis for all three complexes, were grown by liquid diffusion of *i*-Pr<sub>2</sub>O into a MeCN solution of the compound. A summary of the crystal data, data collection, and refinement parameters for the three complexes ([DB24C8·2-H][PF<sub>6</sub>], [BPP34C10·(2-H)<sub>2</sub>][PF<sub>6</sub>]<sub>2</sub>, and [1/5-DN38C10·(2-H)<sub>2</sub>][PF<sub>6</sub>]<sub>2</sub>) is given in Table 4. All three structures were solved by direct methods and were refined by full-matrix least-squares data based on  $F^2$ . All major occupancy non-hydrogen atoms were refined anisotropically, the minor occupancy atoms isotropically. The positions of the hydrogen atoms on the NH<sub>2</sub><sup>+</sup> centers were located from  $\Delta F$  maps and then optimized; the remaining hydrogen atoms were assigned isotropic thermal parameters,  $U(H) = 1.2U_{eq}(C,N)$ , [ $U(H) = 1.5U_{eq}(C-Me)$ ], and were allowed to ride on the parent C/N atoms. In both [DB24C8·2-H][PF<sub>6</sub>] and [BPP34C10·(2-H)<sub>2</sub>][PF<sub>6</sub>]<sub>2</sub>, one of the

PF<sub>6</sub><sup>-</sup> anions was disordered and alternate partial occupancy orientations [60:40 in [DB24C8·2-H][PF<sub>6</sub>] and 66:34 in [BPP34C10·(2-H)<sub>2</sub>][PF<sub>6</sub>]<sub>2</sub>] were identified. In [BPP34C10·(2-H)<sub>2</sub>][PF<sub>6</sub>]<sub>2</sub>, the benzyl ring of the cation was disordered over two (55:45 occupancy) positions. Also, in [BPP34C10·(2-H)<sub>2</sub>][PF<sub>6</sub>]<sub>2</sub>, a full occupancy included MeCN and a CHCl<sub>3</sub> solvent molecule were found. Computations were carried out using the SHELXT PC program system.<sup>24</sup> The crystallographic data (excluding structure factors) for the structures reported in Table 4 have been deposited with the Cambridge Crystallographic Data Centre as supplementary publication number (CDC-100764). Copies of the data can be obtained free of charge on application to the Director, CCDC, 12 Union Road, Cambridge, CB12 1EZ, UK (Fax, Int Code + (1223) 336 0033; e-mail, teched@chemcrs.cam.ac.uk).

(24) SHELXTL PC version 5.03, Siemens Analytical X-Ray Instruments Inc., Madison, WI, 1994.

**Acknowledgment.** This work was supported by MURST, CNR (Progetto Strategico Tecnologie Chimiche Innovative), and University of Bologna (Funds for Selected Topics) in Italy and by the EC contract FMRX-CT96-0076. We thank Ministerio de Educación y Ciencia (Spain) for a Postdoctoral Fellowship to M.-V.M.-D. and Eusko Jaurlaritza, Hezkuntza, Unibertsitate eta Ikerketa Saila, for a Predoctoral Fellowship to M.G.-L.

**Supporting Information Available:** Spectroscopic data for **2** and **2-H·Cl** and X-ray data for [DB24C8·2-H][PF<sub>6</sub>], [BPP34C10·(2-H)<sub>2</sub>][PF<sub>6</sub>]<sub>2</sub>, and [1/5-DN38C10·(2-H)<sub>2</sub>][PF<sub>6</sub>]<sub>2</sub> (34 pages). See any current masthead page for ordering and Internet access instructions.

JA9715760